

**Interface Modulation of Mo₂C@Foam Nickel via MoS₂ Quantum Dots for
Electrochemical Oxygen Evolution Reaction**

Lei Lei ^{a,b}, Danlian Huang ^{a,b,*}, Cui Lai ^{a,b}, Chen Zhang ^{a,b}, Rui Deng ^{a,b}, Yashi Chen ^{a,b},
Sha Chen ^{a,b}, Wenjun Wang ^{a,b}

^a College of Environmental Science and Engineering, Hunan University, Changsha,
Hunan 410082, China

^b Key Laboratory of Environmental Biology and Pollution Control (Hunan University),
Ministry of Education, Changsha, Hunan 410082, China

Synthesis of MoS₂@Mo₂C@NF: The synthesis of MoS₂@Mo₂C@NF was just adding

* Corresponding author at: College of Environmental Science and Engineering, Hunan University, Changsha, Hunan

410082, China.

Tel.: +86-731-88822754; fax: +86-731-88823701.

E-mail address: huangdanlian@hnu.edu.cn (D.L. Huang).

$\text{Mo}_2\text{C}@\text{NF}$ during the synthesis of MoS_2 powders, so that MoS_2 grew in-situ on $\text{Mo}_2\text{C}@\text{NF}$.

Synthesis of MoS_2 QDs@NF: The synthesis of MoS_2 QDs@NF was similar to MoS_2 QDs@ $\text{Mo}_2\text{C}@\text{NF}$ except that $\text{Mo}_2\text{C}@\text{NF}$ was replaced by a bare NF.

Synthesis of MoS_2 QDs@ Mo_2C : The mixture of 0.05 g $(\text{NH}_4)_6\text{Mo}_7\text{O}_{24}$ and 0.05 g $\text{Na}_3\text{C}_6\text{H}_5\text{O}_7 \cdot 2\text{H}_2\text{O}$ were ground to fine powders. Afterwards, the Mo_2C was obtained by calcinating above-mentioned powders at 500°C under Ar for 1 h at a rate of 5°C min⁻¹. Then, ~50 mg of the as-prepared Mo_2C was added into the collected MoS_2 sheets supernatant (70 mL), and was transferred into a 100 ml of Teflon-lined stainless-steel autoclave and was heated at 140°C for 24 h, the MoS_2 QDs@ Mo_2C was obtained.

Preparation of MoS_2 QDs@ Mo_2C and Ru_2O electrodes: The MoS_2 QDs@ Mo_2C and Ru_2O electrodes were prepared by binding the prepared MoS_2 QDs@ Mo_2C and commercial RuO_2 powders onto the bare NF surface using isopropanol and 5 wt% Nafion solution (DuPont, USA) as dispersing agent and binding agent, respectively. In detail, ~2.35 mg MoS_2 QDs@ Mo_2C powders and ~2.35 mg RuO_2 powders were added respectively into a mixture of isopropanol, Nafion and deionized water (0.31/0.62/0.07 volume ratio), and blended to obtain a pasty. The resultant pasty was incorporated onto the NF surface and dried at room temperature to obtain MoS_2 QDs@ Mo_2C and Ru_2O electrodes. For convenience, the electrodes were labeled as MoS_2 QDs@ Mo_2C -bound NF and $\text{RuO}_2@\text{NF}$, respectively. The quantification in the material preparation process was optimized, and the catalyst synthesis was subjected to at least five parallel

experiments to obtain reliable loading data.

Density functional theory calculation

The plane-waves cutoff energy of 330 eV and the conjugate gradient algorithm were selected to assess the electronic ground state with a convergence threshold of 2.0×10^{-6} eV atom $^{-1}$. The tolerance for structural optimization was fixed at 2.0×10^{-5} eV atom $^{-1}$ for energy and 0.05 eV Å $^{-1}$ for force. All of the structures were fully optimized and relaxed to the ground state.

The OER can proceed by the following steps in the alkaline medium:



M referred to the catalyst. Step 1 represented the adsorption and discharge of OH $^-$ at catalyst surface to generate adsorbed OH species. In the step 2, the OH $^-$ interacted with the adsorbed OH species to create adsorbed atomic O and H₂O followed the release of an electron. In the step 3, the OH $^-$ combined with an adsorbed O atom to produce adsorbed OOH species. In the step 4, the OOH species interacted with additional OH $^-$ anions to generate adsorbed O₂ and H₂O molecules followed the release of an electron. Finally, the step 5 presented desorption of the adsorbed O₂ molecule.

The activity of OER was incarnated by the Gibbs free energy change (ΔG_i):

$$\Delta G_i = \Delta E_i + \Delta ZPE_i - T\Delta S_i - neU - 2.303k_B T \text{pH} \quad (6)$$

where ΔG_i represented the variations of the free energy at i th reaction step. ΔG of each reaction step was assessed based on computational hydrogen electrode (CHE) model. ΔE was the reaction energy computed directly from the DFT calculations. The zero-point energy corrections (ΔZPE) and the entropy changes ($T\Delta S$) were obtained from vibrational frequency calculations and standard tables for gas-phase molecules, at 1 bar and 300 K. $T\Delta S$ was approximately -0.2 eV. $-neU$ represented the effect of the external potential for the electrochemical step, where n was the number of transferred electrons and U was the electrode potential relative to the standard hydrogen electrode. k_B was the Boltzmann constant. The vibrational frequency analyses of the gas-phase molecules and adsorbed species were implemented specifically to achieve ZPE . The MoS₂ QDs were fixed assuming that they encountered relatively minor vibrations [1].

The standard equilibrium potential for DFT computations of the overall reaction is $E^0 = 1.23$ vs RHE. The binding energy of intermediates in the model is defined in equilibrium potential (E_i^0) of each elementary electron-transfer (ET) step, as following formula: $E_i^0 = \Delta G_i^0/e$, where i refers to sequence number of elementary ET steps and e is the elementary charge. ΔG_i^0 (in eV) is the reaction free energy of the elementary ET step, which is determined by the binding energy of intermediates. In our work, the equilibrium potential of rate-determining step is defined by $E_{\text{OER}}^0 = \text{Max}(E_i^0)$ [2].

Table S1 Measurements of catalyst loading (mg cm⁻²).

| Catalyst | 1# (mg) | 2# (mg) | 3# (mg) | 4# (mg) | 5# (mg) | Average loading (mg cm ⁻²) |
|---|------------|------------|------------|------------|------------|---|
| Bare NF | 186.4 | 186.9 | 182.1 | 185.1 | 183.7 | |
| MoS ₂ QDs@Mo ₂ C@NF | 202.5 | 205.0 | 196.2 | 217.2 | 197.4 | ~ 2.35 |

Note: The total surface area of the material is $\sim 8 \text{ cm}^2$ assuming that the whole material surface is catalytically active toward the OER.

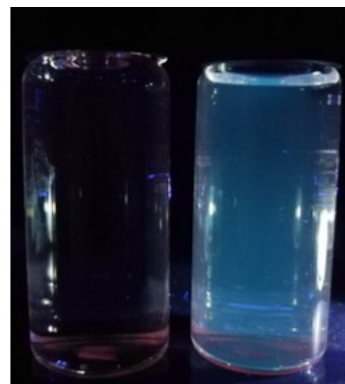


Fig. S1 photograph of H₂O (left) and MoS₂ QDs (right) solutions.

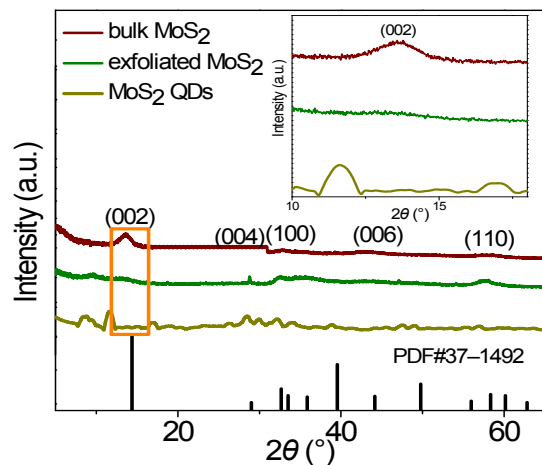


Fig. S2 XRD patterns of MoS₂-based samples. The inset showed the enlarged view of the orange area. The standard card of MoS₂ (PDF#37-1492) was presented for

comparison.

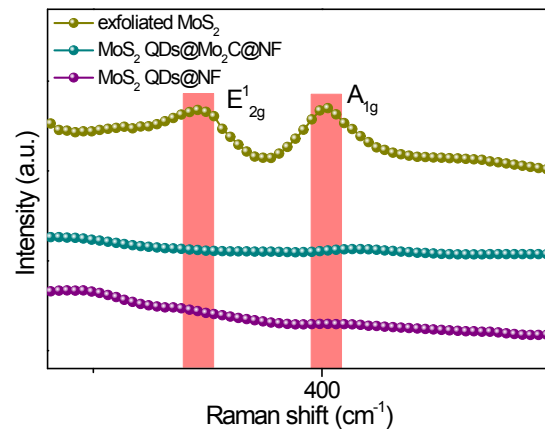


Fig. S3 Enlarged Raman spectrums of exfoliated MoS₂, MoS₂ QDs@Mo₂C@NF and MoS₂ QDs@NF in the pink area of Fig. 1d.

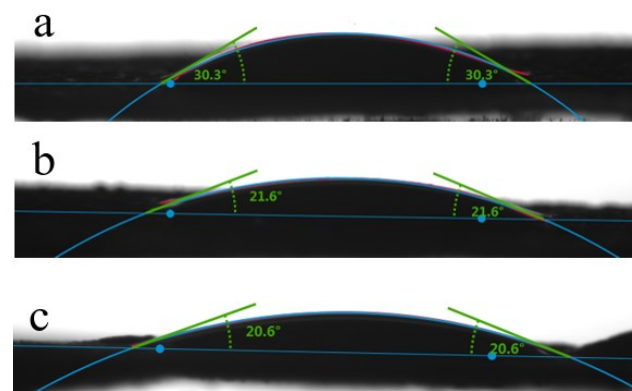


Fig. S4 Static contact angle measurements of (a) Mo₂C@NF, (b) MoS₂ QDs@NF and (c) MoS₂ QDs@Mo₂C@NF.

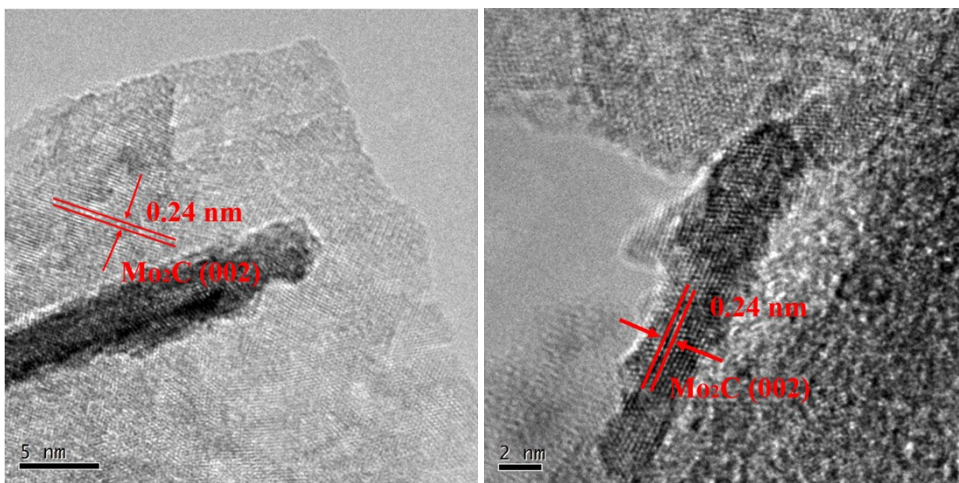


Fig. S5 HRTEM images of (left) Mo₂C@NF and (right) Mo₂C@NF after the hydrothermal process at 200°C for 20 h.

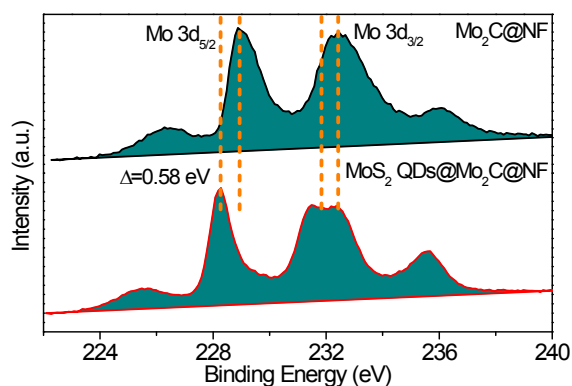


Fig. S6 Mo 3d XPS spectra of Mo₂C@NF and MoS₂ QDs@Mo₂C@NF.

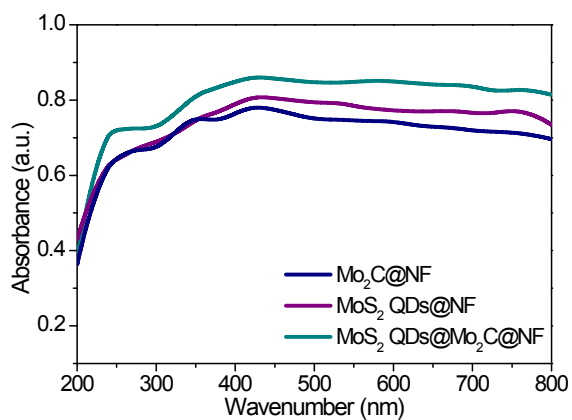


Fig. S7 UV-vis DRS of Mo₂C@NF, MoS₂ QDs@NF and MoS₂ QDs@Mo₂C@NF.

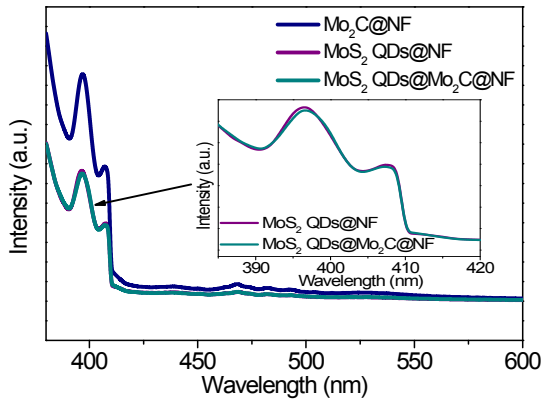


Fig. S8 PL spectra of $\text{Mo}_2\text{C}@\text{NF}$, MoS_2 QDs@NF and MoS_2 QDs@ $\text{Mo}_2\text{C}@\text{NF}$.

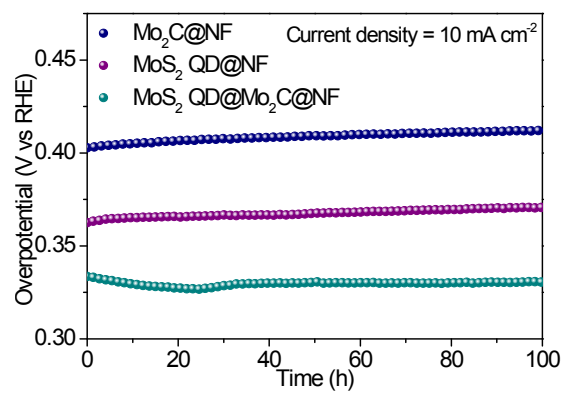


Fig. S9 Chronopotentiometry curves at current density of 10 mA cm^{-2} .

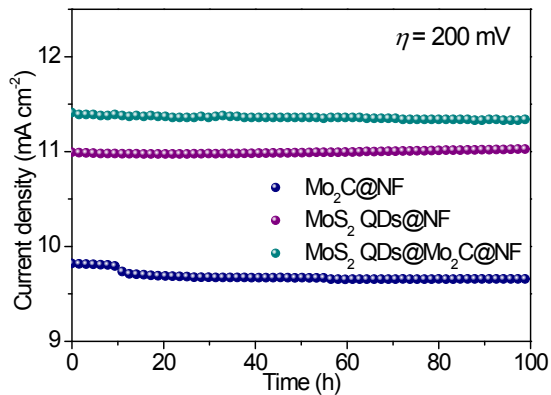


Fig. S10 Chronoamperometry curves under 200 mV static overpotential.

Table S2 Calculated values of the j_0 of various catalysts.

| Catalyst | $\text{Log}(j (\text{mA cm}^{-2}))$ at $\eta=0 \text{ V}$ | $j_0 (\text{mA cm}^{-2})$ |
|---------------------------------|---|---------------------------|
| $\text{Mo}_2\text{C}@\text{NF}$ | -2.13 | 7.4×10^{-3} |

| | | |
|---|-------|-------|
| MoS ₂ QDs@NF | -2.0 | 0.01 |
| MoS ₂ QDs@Mo ₂ C@NF | -1.83 | 0.015 |
| RuO ₂ @NF | -1.67 | 0.021 |

Table S3 Comparison of OER performance of MoS₂ QDs@Mo₂C@NF with reported MoS₂- or Mo₂C-based electrocatalysts in 1.0 M KOH.

| Catalyst | Loading (mg cm ⁻²) | η (mV) at $j=10$ mA | Tafel slope (mV dec ⁻¹) | Reference |
|--|--------------------------------|------------------------------------|-------------------------------------|-----------|
| MoS ₂ /Co ₉ S ₈ /Ni ₃ S ₂ /Ni | 1.86 | 166 | 58 | [3] |
| Co ₃ O ₄ @MoS ₂ /CC | 3.5 | 269 | 58 | [4] |
| Co ₃ S ₄ @MoS ₂ | 0.283 | 280 | 43 | [5] |
| oxygenated-CoS ₂ -MoS ₂ | 1.0 | 272 | 45 | [6] |
| MoS ₂ /NiS NCs | 4.9 | 271 | 53 | [7] |
| Co covalently doped MoS ₂ | 2.0 | 260 | 85 | [8] |
| MoS ₂ /Fe ₅ Ni ₄ S ₈ /FeNi foam | 0.153 | 204 | 28.6 | [9] |
| Ni ₃ S ₂ @MoS ₂ /FeOOH | 2 | 234 | 49 | [10] |
| MoO _x @N-doped MoS _{2-x} | 0.36 | 270 | 61 | [11] |
| MoS ₂ /NiFe-LDH | 0.21 | 210 | 46 | [12] |
| Co ₃ O ₄ /MoS ₂ | 2 | 230 ($j=20$ mA cm ⁻²) | 45 | [13] |
| MoS ₂ @CoNi-ZIF | 0.143 | 340 | 61 | [14] |
| Co ₄ S ₃ /Mo ₂ C-NSC | 0.425 | 268 | 61.2 | [15] |
| Co _{0.1} - β -Mo ₂ C@NC | 0.28 | 262.2 | 28.8 | [16] |
| Mo ₂ C@NC/Co@NG | 0.18 | 424 | 51 | [17] |
| Co/ β -Mo ₂ C@N-CNT | 0.014 | 356 | 67 | [18] |
| Co-NC@Mo ₂ C | 0.83 | 347 | 61 | [19] |
| B,N:Mo ₂ C@BCN NPs | 1.0 | 290 | 61 | [20] |
| Co-Mo ₂ C NPs | 0.24 | 347 | 38 | [21] |
| Co ₉ S ₈ -NSC@Mo ₂ C | 0.425 | 293 | 59.7 | [22] |
| Co ₂ P/Mo ₂ C/Mo ₃ Co ₃ C@C | 0.80 | 362 | 82 | [23] |

| | | | | |
|---|------|-----|----|-----------|
| Ni/Ni ₂ P/Mo ₂ C@C | 0.30 | 368 | 75 | [23] |
| MoS ₂ QDs@Mo ₂ C@NF | 2.35 | 110 | 57 | This work |

Table S4 Resistance fitted according to the Nyquist plots of different samples.

| Catalyst | R_s (Ω) | R_{ct} (Ω) |
|---|--------------------|-----------------------|
| Mo ₂ C@NF | 0.11717 | 1.846 |
| MoS ₂ QDs@NF | 0.12621 | 1.827 |
| MoS ₂ QDs@Mo ₂ C@NF | 0.12403 | 1.704 |

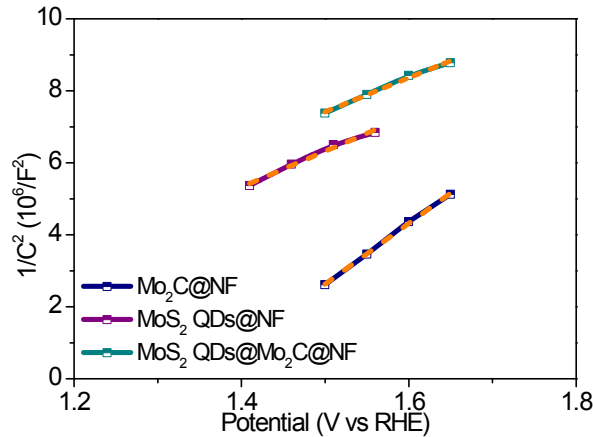


Fig. S11 Mott-Schottky plots of Mo₂C@NF, MoS₂ QDs@NF and MoS₂ QDs@Mo₂C@NF.

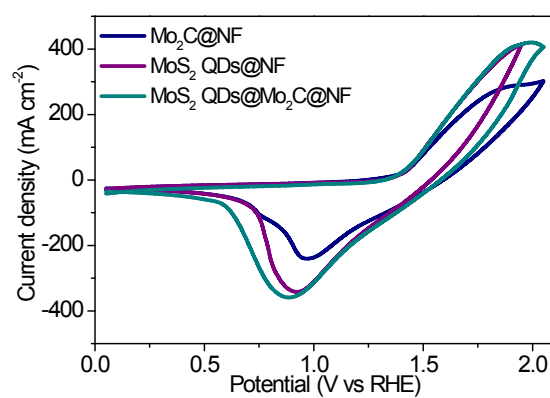


Fig. S12 The CV curves in 1.0 M KOH for Mo₂C@NF, MoS₂ QDs@NF and MoS₂ QDs@Mo₂C@NF.

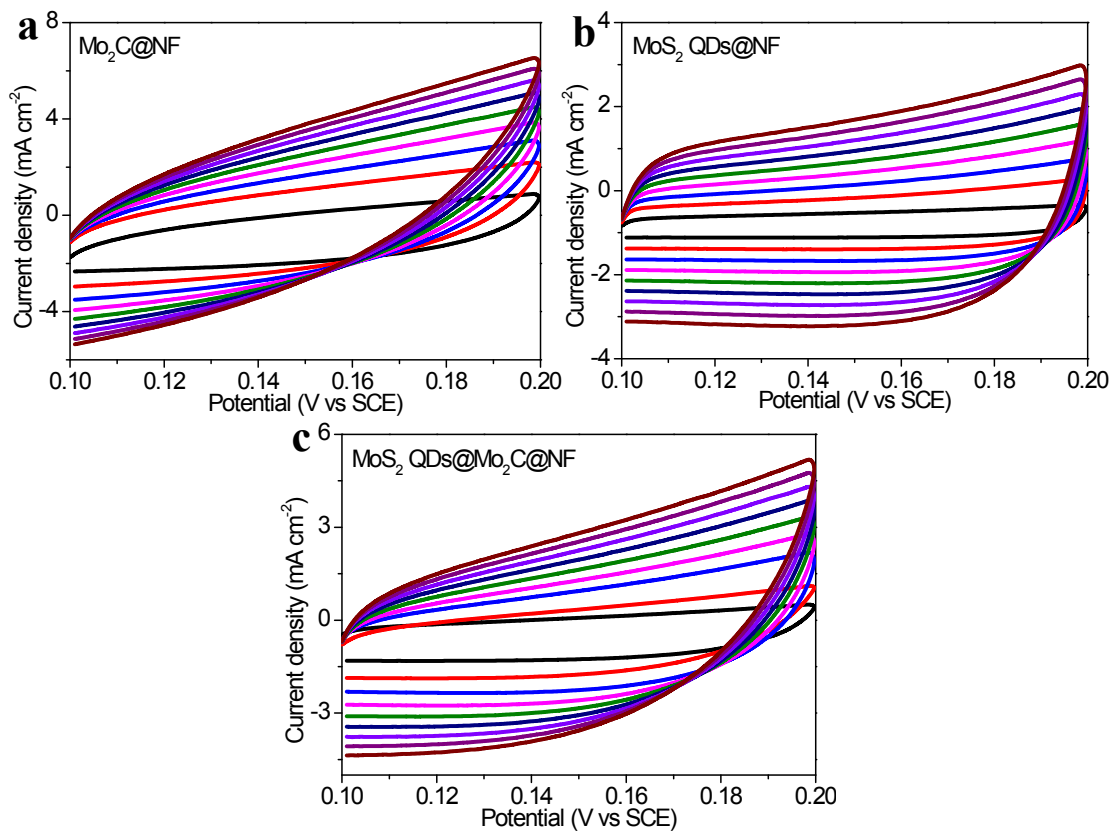


Fig. S13 CV for different electrocatalysts at different scan rates of 20, 40, 60, 80, 100, 120, 140, 160, 180 mV s⁻¹ from inner to out, respectively. **(a)** Mo₂C@NF, **(b)** MoS₂ QDs@NF and **(c)** MoS₂ QDs@Mo₂C@NF.

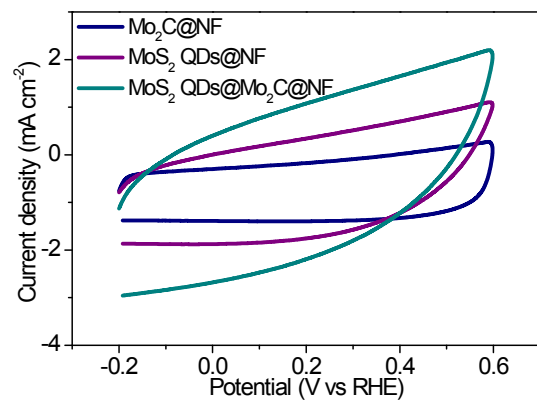


Fig. S14 The CV curves in 1.0 M PBS for Mo₂C@NF, MoS₂ QDs@NF and MoS₂ QDs@Mo₂C@NF.

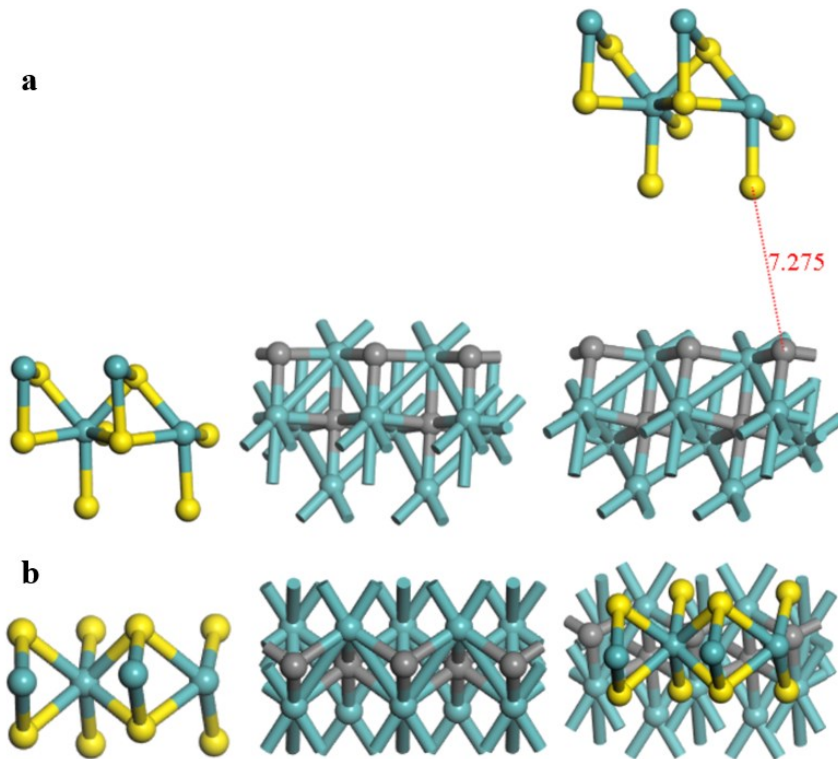
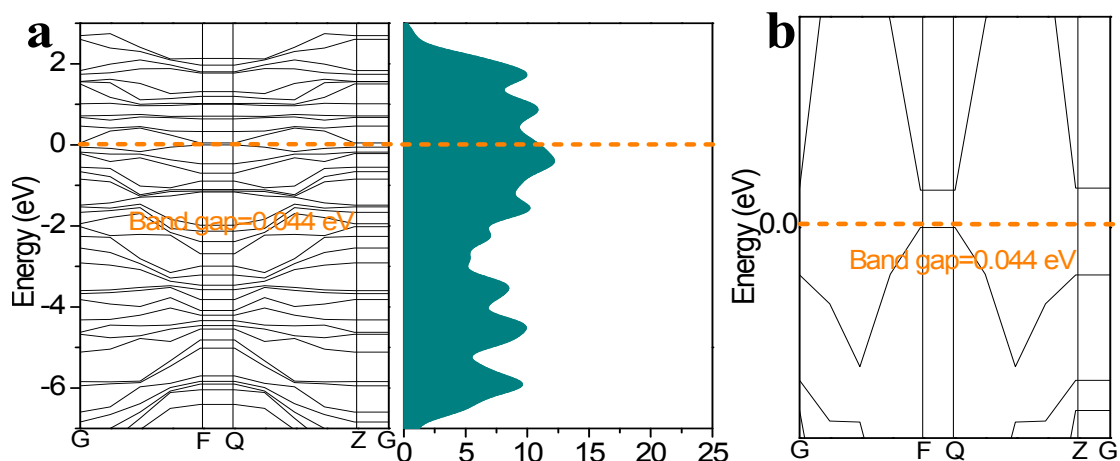


Fig. S15 (a) Side-view and (b) top-view of a part of the optimized MoS₂ QDs@NF (left), Mo₂C@NF (middle) and MoS₂ QDs@Mo₂C@NF (right) (NF is omitted) according to the (100) basal plane for the calculation. Dark cyan, yellow and gray balls represent Mo, S and C atoms, respectively.



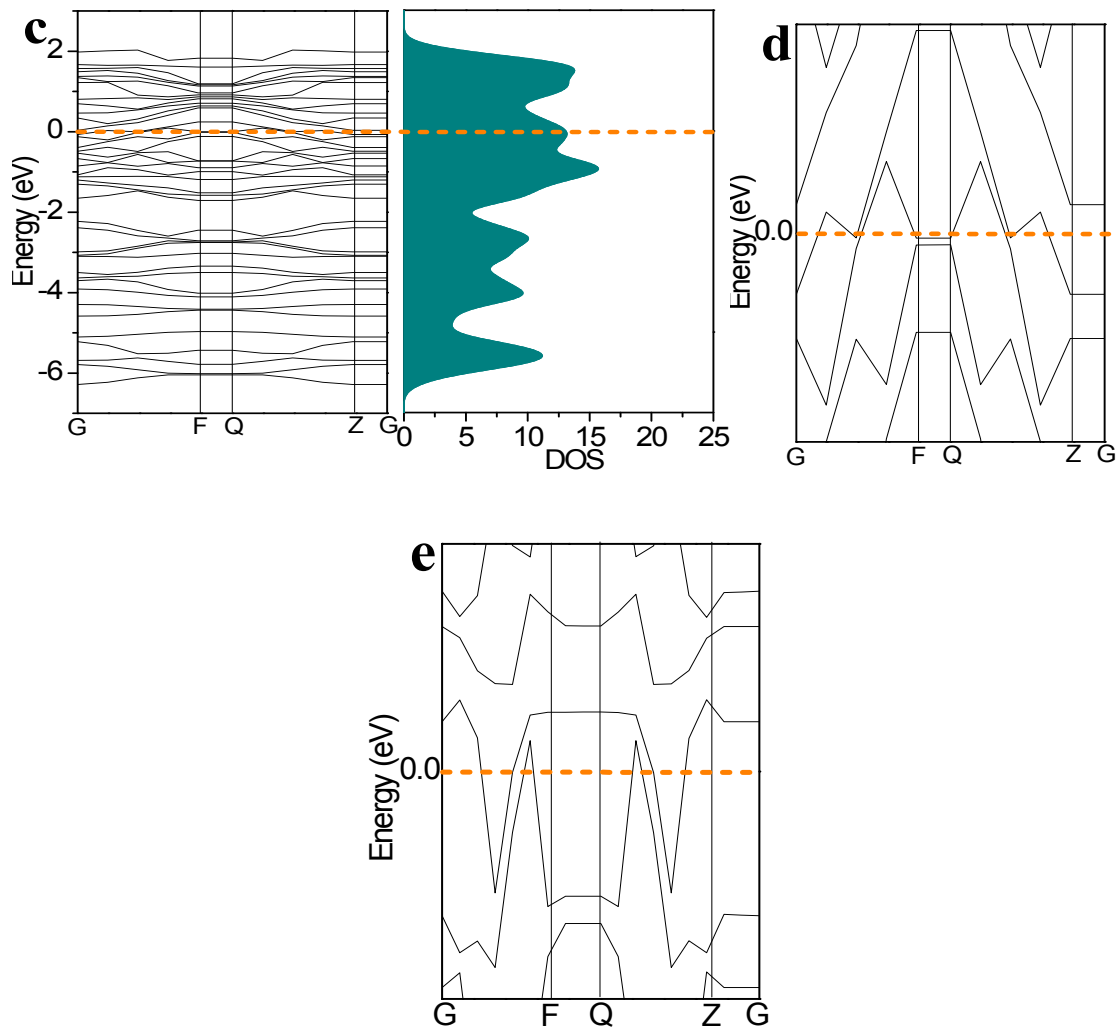
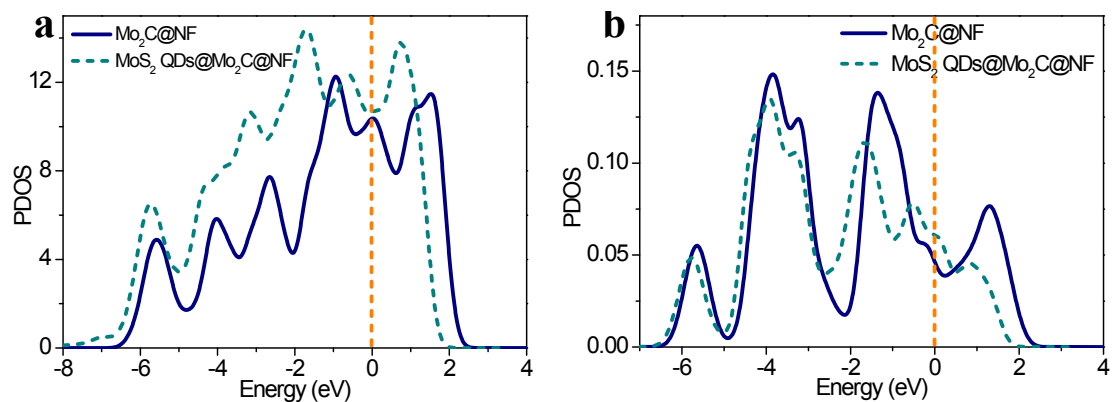


Fig. S16 Band structure and corresponding TDOS of **(a)** MoS₂@NF and **(c)** Mo₂C@NF. **(b)** and **(d)** are enlarged views near horizontal dashed lines in **(a)** and **(c)**, respectively. **(e)** is the enlarged view near horizontal dashed lines in Fig. 7c. The horizontal dashed lines indicate the Fermi level.



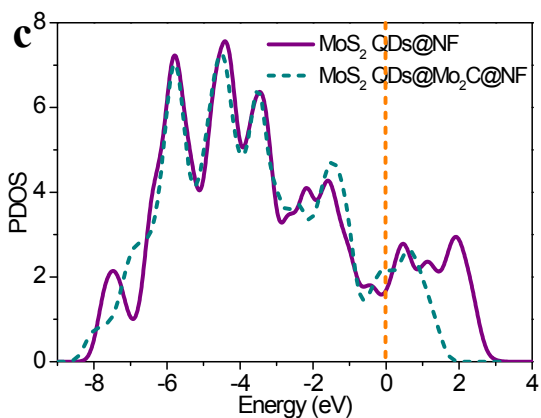


Fig. S17 PDOS plots for **(a)** Mo atom and **(b)** C atom in $\text{Mo}_2\text{C}@\text{NF}$ and MoS_2 QDs@ $\text{Mo}_2\text{C}@\text{NF}$. **(c)** PDOS plots for S atom in MoS_2 QDs@NF and MoS_2 QDs@ $\text{Mo}_2\text{C}@\text{NF}$. The vertical dashed lines indicate the Fermi level.

Reference

- [1] B. Mohanty, M. Ghorbani-Asl, S. Kretschmer, A. Ghosh, P. Guha, S. K. Panda, B. Jena, A.V. Krasheninnikov and B.K. Jena, ACS Catal., 2018, 8, 1683-1689.
- [2] H. B. Tao, J. Zhang, J. Chen, L. Zhang, Y. Xu, J. G. Chen and B. Liu, J. Am. Chem. Soc., 2019, 141, 13803-13811.
- [3] Y. Yang, H. Yao, Z. Yu, S. M. Islam, H. He, M. Yuan, Y. Yue, K. Xu, W. Hao, G. Sun, H. Li, S. Ma, P. Zapal and M. G. Kanatzidis, J. Am. Chem. Soc., 2019, 141, 10417-10430.
- [4] J. Liu, J. Wang, B. Zhang, Y. Ruan, H. Wan, X. Ji, K. Xu, D. Zha, L. Miao and J. Jiang, J. Mater. Chem. A, 2018, 6, 2067-2072.
- [5] Y. Guo, J. Tang, Z. Wang, Y. Kang, Y. Bando and Y. Yamauchi, Nano Energy, 2018, 47, 494-502.
- [6] J. Hou, B. Zhang, Z. Li, S. Cao, Y. Sun, Y. Wu, Z. Gao and L. Sun, ACS Catal.,

2018, 8, 4612-4621.

- [7] Z. Zhai, C. Li, L. Zhang, H. Wu, L. Zhang, N. Tang, W. Wang and J. Gong, *J. Mater. Chem. A*, 2018, 6, 9833-9838.
- [8] Q. Xiong, Y. Wang, P. Liu, L. Zheng, G. Wang, H. Yang, P. Wong, H. Zhang and H. Zhao, *Adv. Mater.*, 2018, 30, 1801450.
- [9] Y. Wu, F. Li, W. Chen, Q. Xiang, Y. Ma, H. Zhu, P. Tao, C. Song, W. Shang, T. Deng and J. Wu, *Adv. Mater.*, 2018, 30, 1803151.
- [10] M. Zheng, K. Guo, W. Jiang, T. Tang, X. Wang, P. Zhou, J. Du, Y. Zhao, C. Xu and J. Hu, *Appl. Catal. B-Environ.*, 2019, 244, 1004-1012.
- [11] Y. Wang, S. Liu, X. Hao, S. Luan, H. You, J. Zhou, D. Song, D. Wang, H. Li and F. Gao, *J. Mater. Chem. A*, 2019, 7, 10572-10580.
- [12] P. Xiong, X. Zhang, H. Wan, S. Wang, Y. Zhao, J. Zhang, D. Zhou, W. Gao, R. Ma, T. Sasaki and G. Wang, *Nano Lett.*, 2019, 19, 4518-4526.
- [13] A. Muthurasu, V. Maruthapandian and H. Y. Kim, *Appl. Catal. B-Environ.*, 2019, 248, 202-210.
- [14] Y. Liu, B. Hu, S. Wu, M. Wang, Z. Zhang, B. Cui, L. He and M. Du, *Appl. Catal. B-Environ.*, 2019, 258, 117970.
- [15] Y. Liu, X. Luo, C. Zhou, S. Du, D. Zhen, B. Chen, J. Li, Q. Wu, Y. Iru and D. Chen, *Appl. Catal. B-Environ.*, 2020, 260, 118197.
- [16] X. Zhu, X. Zhang, L. Huang, Y. Liu, H. Zhang and S. Dong, *Chem. Commun.*,

2019, 55, 9995-9998.

[17] Y. Wang, K. Li, F. Yan, C. Li, C. Zhu, X. Zhang and Y. Chen, *Nanoscale*, 2019, 11, 12563-12572.

[18] T. Ouyang, Y. Ye, C. Wu, K. Xiao and Z. Liu, *Angew. Chem. Int. Ed.*, 2019, 58, 4923-4928.

[19] Q. Liang, H. Jin, Z. Wang, Y. Xiong, S. Yuan, X. Zeng, D. He and S. Mu, *Nano Energy*, 2019, 57, 746-752.

[20] M. A. R. Anjum, M. H. Lee and J. S. Lee, *ACS Catal.*, 2018, 8, 8296-8305.

[21] M. Kim, S. Kim, D. Song, S. Oh, K. J. Chang and E. Cho, *Appl. Catal. B-Environ.*, 2018, 227, 340-348.

[22] X. Luo, Q. Zhou, S. Du, J. Li, J. Zhong, X. Deng and Y. Liu, *ACS Appl. Mater. Interfaces*, 2018, 10, 22291-22302.

[23] X. Li, X. Wang, J. Zhou, L. Han, C. Sun, Q. Wang and Z. Su, *J. Mater. Chem. A*, 2018, 6, 5789-5796.